First publ. in: Journal of Applied Physics 101 (2007), 073904

Defect induced low temperature ferromagnetism in $Zn_{1-x}Co_xO$ films

E. Biegger,[a] M. Fonin, and U. Rüdiger
Fachbereich Physik, Universität Konstanz, 78457 Konstanz, Germany

N. Janßen, M. Beyer, T. Thomay, and R. Bratschitsch
Fachbereich Physik, Universität Konstanz and Center for Applied Photonics, 78457 Konstanz, Germany

Yu. S. Dedkov
Institut für Festkörperphysik, Technische Universität Dresden, 01062 Dresden, Germany

We present a detailed study on the structural, magnetic, and optical properties, as well as the electronic structure of epitaxial Co-doped ZnO films prepared by magnetron sputtering. Different preparation conditions were implemented in order to control the concentration of oxygen vacancies in the ZnO host lattice. Magnetization measurements indicate ferromagnetic behavior at low temperature for samples prepared at oxygen-poor conditions whereas the samples prepared at oxygen-rich conditions show extremely small ferromagnetic signal corroborating that ferromagnetism in $Zn_{1-x}Co_xO$ correlates with the presence of the oxygen-related defects. X-ray absorption spectroscopy (XAS) at the Co $L_{2,3}$ edge together with optical transmittance measurements show that Co ions are present in the high-spin Co^{2+} (d^7) state under tetrahedral symmetry indicating a proper incorporation in the ZnO host lattice. Comparison of the O K edge XAS spectra of the samples prepared at different conditions show substantial changes in the spectral line shape which are attributed to the presence of lattice defects such as oxygen vacancies in the ferromagnetic oxygen-poor Co-doped ZnO samples. Our findings indicate that the ferromagnetic properties of Co-doped ZnO samples are strongly correlated with the presence of oxygen vacancies in the ZnO lattice supporting the spin-split impurity band model.

I. INTRODUCTION

Diluted magnetic semiconductors (DMS) have recently become the subject of an intensive research due to the possibility to utilize both charge and spin degrees of freedom in the same material, which allows to design a new generation of spintronic devices with enhanced functionalities. Investigations on the DMS were originally inspired by the discovery of spontaneous low temperature ferromagnetism in Mn-doped GaAs exhibiting a Curie temperature (T_C) of about 110 K.[1] Recent theoretical studies on the basis of Zener's model showed that transition-metal-doped wide-gap semiconductors, among them Mn-doped ZnO, are promising candidates for room temperature (RT) ferromagnetism.[2,3] This has stimulated numerous experimental works on the preparation of RT ferromagnetic transition-metal-doped ZnO.[4] In the early work of Ueda *et al.*[5] ferromagnetic behavior with T_C above RT for the Co-doped ZnO films grown by the pulsed laser deposition (PLD) technique was observed. Following this first study several groups reported on Co-doped ZnO exhibiting T_C well above RT.[4,6,7] However, other studies showed only very low magnetic ordering temperatures in $Zn_{1-x}Mn_xO$ (Refs. 8 and 9) or even the absence of ferromagnetism in the $Zn_{1-x}Co_xO$ samples prepared by different techniques.[10–12] These controversial experimental results give an indication that ferromagnetism in DMS is very sensitive to the preparation method and preparation conditions. Moreover, even magnetic properties of $Zn_{1-x}Co_xO$ samples prepared by the same deposition technique with the same cobalt concentration show a lack of reproducibility.

The origin of ferromagnetic behavior in Co-doped ZnO is far from being understood with some reports attributing ferromagnetism to ferromagnetic Co clusters incorporated into the ZnO matrix[13] or substitution by Co atoms in the ZnO lattice.[5,7] Other studies show that occupation of the substitutional sites by Co atoms is not a sufficient condition for ferromagnetic behavior.[14] In order to explain the origin of ferromagnetism in ZnO doped with transition metal atoms several possible mechanisms were introduced. Dietl *et al.*[2] proposed ferromagnetism due to the exchange interaction mediated by carriers in the valence or conduction band and the localized moment of the transition-metal ions. A double exchange mechanism in which hopping of 3d electrons results in ferromagnetic behavior was considered in a recent *ab initio* electronic structure calculation.[15]

In addition to the transition metal doping effect, structural defects such as oxygen vacancies were proposed to influence the ferromagnetic state of the oxide DMS. For example, theoretical studies suggest that oxygen vacancies can alter the band structure of a host oxide and make a significant contribution to the ferromagnetism.[16,17] The formation of a shallow spin-split impurity band upon coalescence of bound magnetic polarons (BMPs) constituted by donor defects has also been proposed to explain the origin of RT ferromagnetism for oxide DMS.[4] Recently, a number of experiments showed the correlation between the ferromagnetic behavior

[a]Electronic mail: erwin.biegger@uni-konstanz.de

and the concentration of structural defects, either Zn interstitials[18,19] or oxygen vacancies,[20,21] incorporated into the ZnO host lattice giving an evidence that ferromagnetism in Co-doped ZnO is mediated by donor-bound carriers.

In this study, Co-doped ZnO films have been prepared by a magnetron sputtering technique to investigate the structural, magnetic, optical, and electronic properties of the DMS $Zn_{1-x}Co_xO$. Control over the oxygen vacancy concentration in the ZnO host lattice was achieved by using different preparation conditions such as Ar and Ar/O_2 sputtering in conjunction with postannealing. Magnetization measurements indicate weak ferromagnetism at low temperature for samples prepared at oxygen poor conditions, whereas the samples prepared at oxygen rich conditions show extremely small if any ferromagnetic signature. X-ray absorption spectroscopy (XAS) at the Co $L_{2,3}$ absorption edge and optical transmittance measurements have been performed to identify the oxidation state and site symmetry of Co in the ZnO host lattice. In case of ferromagnetic Co-doped ZnO samples both photoluminescence (PL) and O *K* XAS spectra show features which could be related to oxygen defects.

II. EXPERIMENT

Epitaxial $Zn_{1-x}Co_xO$ (x=0.05 and 0.1) films have been prepared by radio-frequency reactive magnetron sputtering of $[ZnO(20\ Å)/Co(d\ Å)]_{50}$ (d=2 and d=5) multilayers on $Al_2O_3(0001)$ substrates. The variation of the Co content was achieved by sputtering different thicknesses of Co intermediate layers. During the deposition the substrate temperature was kept at about 480 °C. The deposition of ZnO/Co multilayers was performed in a process pressure of about 3×10^{-3} mbar with an Ar (Ar/O_2) ion beam acting alternatively on high purity ZnO and Co targets. Oxygen-poor samples further referred to as *S*1 and oxygen-rich samples further referred to as *S*2 were prepared by sputtering in a pure Ar atmosphere and in an Ar/O_2 mixture with a ratio of 5:2 at the same deposition pressure of 3×10^{-3} mbar, respectively. After the growth the temperature of the samples was maintained at 480 °C for 2 h and then slowly decreased to room temperature. Oxygen-rich samples have been additionally heated *ex situ* in oxygen atmosphere at 600 °C and 1 bar for 2 h. Before the deposition the $Al_2O_3(0001)$ substrates were annealed in oxygen at 1 bar and 800 °C for 4 h which was found to suppress ferromagnetic contributions of the substrate with respect to the grown $Zn_{1-x}Co_xO$ films.

The investigation of the crystallographic structure was done by x-ray diffraction (XRD) using a Siemens diffractometer through $\theta-2\theta$ scans and ω rocking curves. The Co content in the films was verified by means of an energy dispersive x-ray analysis. Magnetic characterization was performed by a superconducting quantum interference device (SQUID) from Quantum Design. In all experiments the magnetic signal of the Al_2O_3 substrates was measured before the film deposition and was subsequently subtracted from the data measured on the $Zn_{1-x}Co_xO$ samples. Photoelectron spectroscopy (PES) as well as XAS experiments were carried out at RT at the RGBL-PGM beamline at BESSY (Berlin). The ultrahigh vacuum (UHV) system with a base pressure of 1×10^{-10} mbar was equipped with a CLAM4 analyzer. The total energy resolution in the x-ray photoelectron spectroscopy measurements was set to 150 meV. The position of the Fermi energy (E_F) was determined form the valence-band spectrum of a polycrystalline Au foil in electrical contact with the sample. All spectra were normalized to the incident photon flux. XAS spectra were collected in the total electron yield mode and normalized to the maximum intensity. The energy resolution in the XAS experiments was set to 100 meV. Before PES and XAS measurements the samples were cleaned in UHV by Ar^+ sputtering.

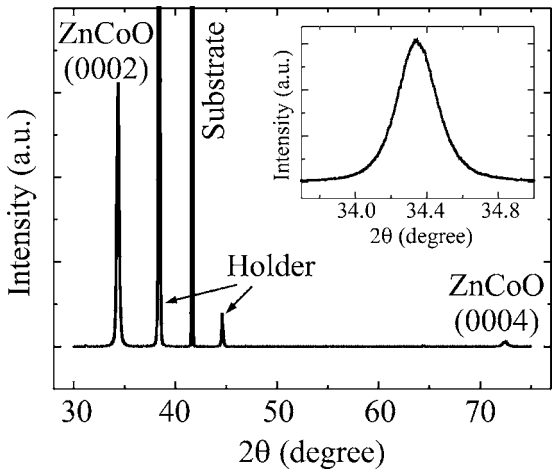

FIG. 1. A typical XRD pattern of the epitaxial $Zn_{0.95}Co_{0.05}O$ film. The inset shows the zoom into the (0002) peak of $Zn_{1-x}Co_xO$.

PL measurements were performed with $Nd:YVO_4$ continuous wave laser (Coherent Verdi V10) at 532 nm. The power of the laser was 10 W and the frequency was doubled with a BBO (Beta-Bariumborat) crystal to 266 nm, resulting in a conversion-factor of 0.08%. Optical transmittance measurements were carried out using a Agilent 8453E ultraviolet-visible spectrometer with a resolution of 1 nm.

III. RESULTS AND DISCUSSION

Figure 1 shows a typical XRD pattern of a 120 nm-thick $Zn_{0.95}Co_{0.05}O$ film prepared on $Al_2O_3(0001)$. Two diffraction peaks were observed at about 34.4° and 72.4° which correspond to the (0002) and (0004) reflections of the hexagonal ZnO wurtzite structure showing the excellent epitaxial quality of the ZnO films with *c*-axis orientation. This is further confirmed by the rocking curves obtained around the (0002) reflection, which show a full width at half maximum (FWHM) of 2.8°.

Magnetization measurements of two sample sets, *S*1 (oxygen-poor) and *S*2 (oxygen-rich), were performed as a function of magnetic field $[M(H)]$ as well as temperature $[M(T)]$. Figure 2(a) shows $M(H)$ curves of the $Zn_{0.9}Co_{0.1}O$ film grown in oxygen-poor conditions measured at 300 K as well as at 5 K. A clear hysteresis loop with a coercive field (H_C) of about 200 Oe can be observed at 5 K. The saturation magnetization (M_s) was estimated to be about 0.05 μ_B/Co at 5 K and 20 kOe, which is much smaller than that expected for Co^{2+} (3 μ_B) corroborating that only a small fraction of the Co atoms contribute to ferromagnetism. Thus most of the

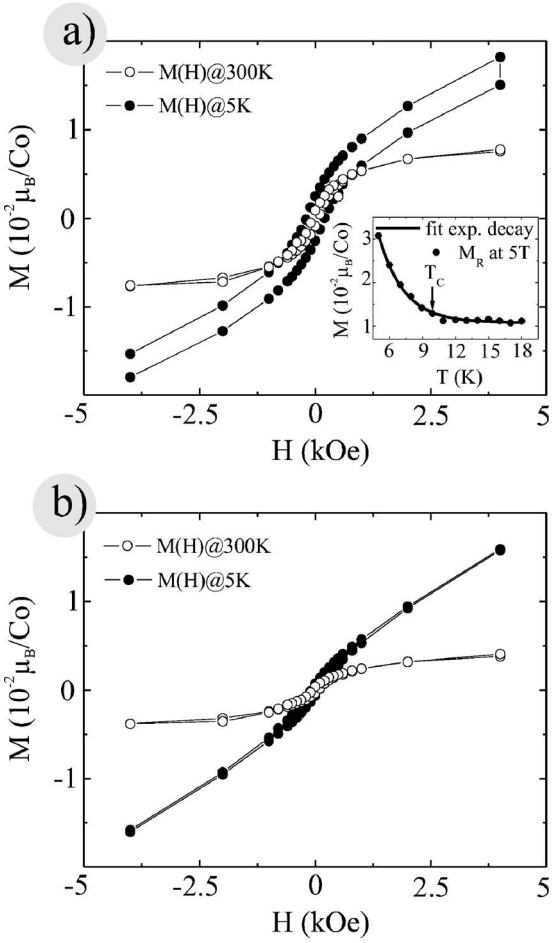

FIG. 2. (a) Magnetization loop of the $Zn_{0.9}Co_{0.1}O$ sample *S*1 grown in oxygen-poor conditions measured at 5 and 300 K. The ferromagnetic loop is closed at 20 kOe. The inset shows the temperature dependent remanent magnetization after saturation in a field of 5 T (solid circles) together with an exponential fit (solid line). (b) Magnetization loop of the $Zn_{0.9}Co_{0.1}O$ sample *S*2 grown in oxygen-rich conditions measured at 5 and 300 K.

Co atoms should be antiferromagnetically coupled at this relatively high Co concentration (about 5%–10%). The inset in Fig. 2(a) shows the temperature dependent magnetization $[M(T)]$ measured upon warming up the sample without magnetic field after saturating it in a 5 T magnetic field. The temperature dependence of the remanent magnetization is comparable to that of In(Mn)As samples.[22] The concave shape of the $M(T)$ remanence measured at zero field can be explained in the framework of polaron percolation in the limit of low carrier density.[23] The driving force behind the ferromagnetic transition is the ordering of impurity spins around the localized carriers to magnetic polarons. The average radius of polarons increases exponential with decreasing temperature.[24] Therefore an exponential fit was performed in order to show an exponential decay of the first order. At a certain temperature it grows large enough that polarons percolate into a infinite cluster which can be attributed to the Curie temperature T_C as shown in the inset of Fig. 2(a). However, since the percolating cluster does not contain a majority of the magnetic impurity and most impurity spins remain free even at a low temperature, these uncoupled spins give rise to the slow saturation of magnetization. Figure 2(b) shows the $M(H)$ curves of the $Zn_{0.9}Co_{0.1}O$ sample *S*2 grown

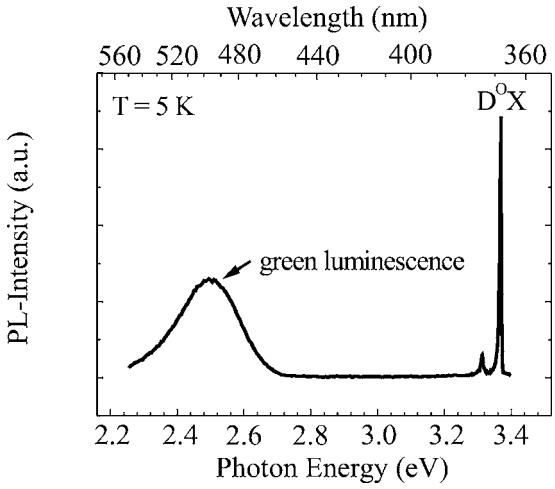

FIG. 3. A typical PL spectrum of a $Zn_{0.95}Co_{0.05}O$ sample. The broad luminescence band around 2.5 eV is attributed to the presence of oxygen vacancies.

in oxygen-rich conditions followed by subsequential annealing in O_2. Coercive field and remanence are very small if any at 5 K as well as at 300 K showing that ferromagnetism is absent in these samples or at least beyond the detection limit of the SQUID magnetometer. Furthermore, zero field cooled (ZFC) and field cooled (FC) measurements have been performed at 10 mT at both samples *S*1 and *S*2 to investigate the possible formation of Co clusters during sample preparation. Contrary to Park *et al.*,[25] no blocking temperature was observed at any sample and ZFC did not differ significantly from FC measurement indicating that Co is distributed in all $Zn_{1-x}Co_xO$ samples homogeneously. Thus, a controlled variation of the magnetic behavior of the $Zn_{1-x}Co_xO$ samples can be achieved by varying of the oxygen content in preparation conditions.

PL together with the optical transmittance measurements have been performed at the Co-doped ZnO samples in order to investigate the optical properties of transparent DMS $Zn_{1-x}Co_xO$. Figure 3 shows a PL spectrum of a $Zn_{0.95}Co_{0.05}O$ sample measured at 5 K. The most intensive luminescence is visible near the band gap region of ZnO at 3.37 eV in agreement with Reynolds *et al.*,[26] and is attributed to the neutral-donor-bound-exciton D^0X recombination. The FWHM was measured to be 6.3 meV. A second smaller peak is observed at lower energies, which is possibly due to the donator-acceptor transitions (D, A).[27] At lower energies, a broad PL band is visible around 2.5 eV. The origin of this green emission has been discussed controversially. Studenikin *et al.*[28] assigned it to a donator-acceptor transition (D, A) from oxygen vacancy (O_V) to Zn vacancies (Zn_V). A transition between Zn_V and Zn interstitials (Zn_i) was suggested by Xu *et al.*[29] Further investigations ascribed the appearance of the green luminescence to transitions involving deep-levels within the band gap associated with oxygen vacancies.[28,30,31]

Figure 4 shows the optical transmittance spectrum of the $Zn_{0.9}Co_{0.1}O$ sample measured at RT. The transmittance increases drastically at the band gap energy around 368 nm corresponding to 3.37 eV. Furthermore, optical absorption lines are visible from 550 to 700 nm, which are attributed to

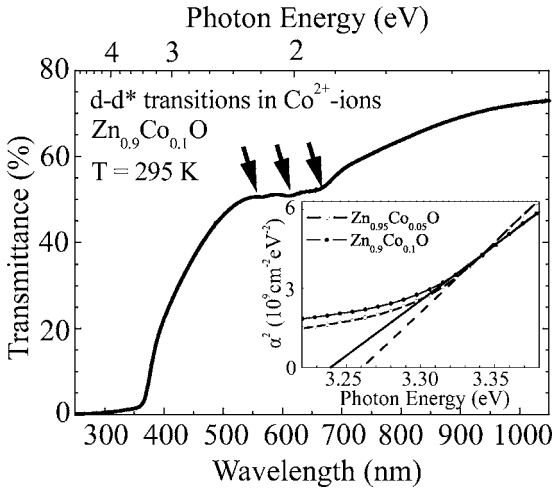

FIG. 4. A typical optical transmittance spectrum of the $Zn_{0.9}Co_{0.1}O$ sample. The spectrum reveals characteristic absorption bands, which are assigned to $d-d^*$ transitions in the Co^{2+} ion substituting Zn^{2+} sites. The inset shows the decreasing band gap energy with the increasing Co concentration.

the Co^{2+} absorption bands, because the $3d$ levels are split in the crystal field of ZnO.[32] These absorption bands are assigned to transitions from the ground state $^4A_2(F)$ to $^2E(G)$ (659 nm), to $^4T_1(P)$ (611 nm), and to $^2A_1(G)$ (566 nm) states, respectively, corresponding to intraionic $d-d^*$ transitions[33] in tetrahedrally coordinated high-spin Co^{2+} ions substituting Zn^{2+} sites in the ZnO host lattice. The experimental results are in good agreement with the theoretical calculations for the d^7 Co^{2+} ions in a tetrahedral coordination.[34] The inset in Fig. 4 shows the squared absorption coefficient α as a function of the photon energy which can be used to extract the band gap energy of the $Zn_{1-x}Co_xO$ samples. The absorption coefficient α can be estimated as

$$\alpha = B\sqrt{(h\nu - E_g)}, \tag{1}$$

with B being a constant, $h\nu$-photon energies, and the band gap energy E_g. The extrapolation of the linear fit gives the value of the band gap at the intersection with the photon energy axis[35] (inset of Fig. 4). For increasing Co concentration, a decreasing band gap energy was observed. This can be explained by the $sp-d$ exchange interaction between the band electrons and the localized d electrons of the Co^{2+} ions substituting the Zn^{2+} sites. The band gap narrowing is in agreement with results of sputtered[36] and PLD grown[37] films due to the incorporation of Co into the ZnO host lattice.

The electronic structure of the Co-doped ZnO were investigated in detail by means of XAS and PES. Figure 5(a) shows XAS spectra of the $Zn_{0.95}Co_{0.05}O$ samples $S1$ and $S2$ measured at Co $L_{2,3}$ absorption edge. The Co $2p_{3/2}$ peak at 778 eV and the Co $2p_{1/2}$ peak at 793 eV are clearly separated by the large $2p$ core-hole spin-orbit interaction. The line shape of XAS spectra from samples $S1$ and $S2$ is clearly different from that of the Co metal showing the absence of any Co clustering which could be expected due to the multilayer growth. Thus these data rule out phase segregation as the source of ferromagnetism in Co-doped ZnO and point to an intrinsic origin. The observed line shape is similar to that of the previously reported spectra from both

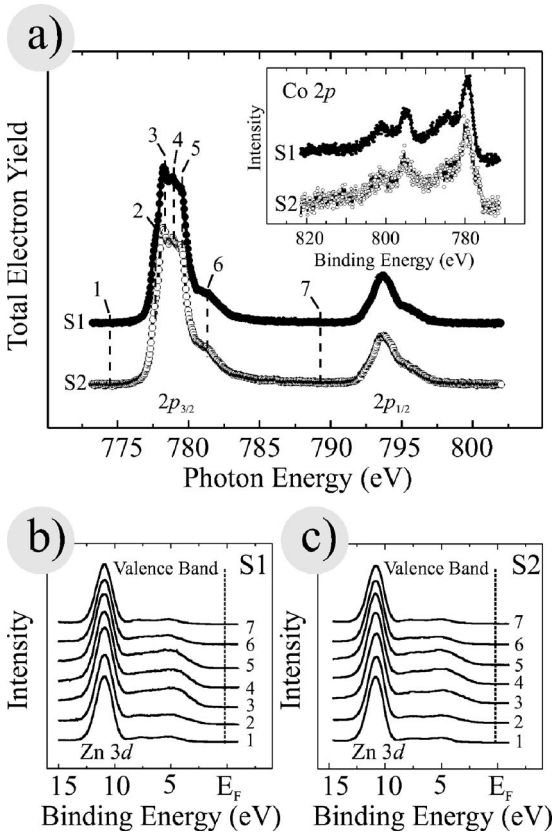

FIG. 5. (a) Co $L_{2,3}$ XAS spectra of the oxygen-poor ($S1$) and oxygen-rich ($S2$) $Zn_{0.95}Co_{0.05}O$ samples. Inset shows the core-level PES spectra of both samples where Co $2p_{1/2}$ and $2p_{3/2}$ peaks are visible. (b) and (c) show resonant PES valence band spectra of samples $S1$ and $S2$, respectively, measured at photon energies marked in (a).

ferromagnetic[38] and nonmagnetic[14] Co-doped ZnO, as well as to several atomic multiplet configuration interaction calculations[14,38,39] confirming that cobalt ions are present in the high-spin Co^{2+} state under tetrahedral coordination indicating a proper incorporation into the ZnO host lattice. Although the samples $S1$ and $S2$ should differ in the oxygen content, only a very small difference in the spectral line shape (intensity of the feature marked as 5 in the XAS spectra) is visible. The inset of Fig. 5(a) shows Co $2p$ core level PES spectra of both $S1$ and $S2$ $Zn_{0.95}Co_{0.05}O$ samples taken at $h\nu = 1000$ eV. The Co $2p$ spectra of both samples are similar to that of CoO supporting the presence of Co^{2+} ions in the samples.

Figures 5(b) and 5(c) show representative valence band photoemission spectra of the $S1$ and $S2$ $Zn_{0.95}Co_{0.05}O$ samples as a function of photon energy including the Co $2p-3d$ excitation threshold. The valence band spectra of $Zn_{0.95}Co_{0.05}O$ are similar to that of ZnO showing a sharp peak at about 11 eV of the binding energy (BE) corresponding to Zn $3d$ states as well as a broad feature between 3 and 8 eV of BE corresponding to O $2p$ band. No photoemission intensity was observed in the E_F region confirming the insulating nature of the samples. Thus the charge carrier mediated ferromagnetism based on the Ruderman–Kittel–Kasuya–Yosida mechanism or related Zener mechanism, in which itinerant free carriers interact with localized d electrons of isolated dopant ions can be ruled out. Figure 6(a)

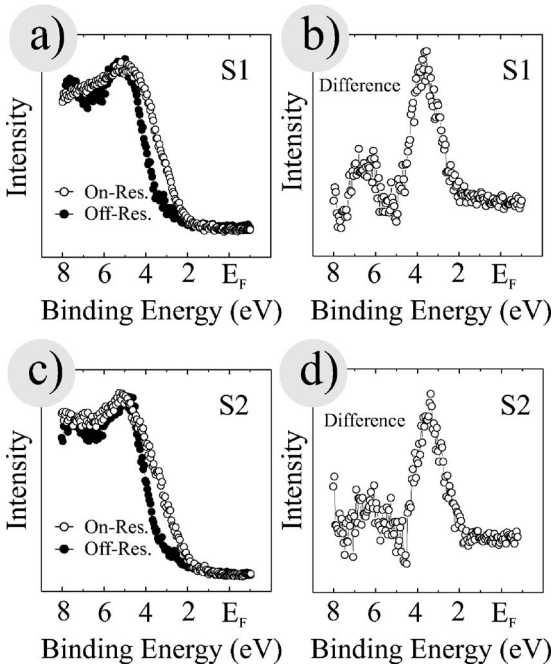

FIG. 6. (a) and (c) show on- and off-resonance spectra of samples *S*1 and *S*2, respectively. (b) and (d) exhibit the difference curve obtained by subtraction of the off- and on-resonance spectra.

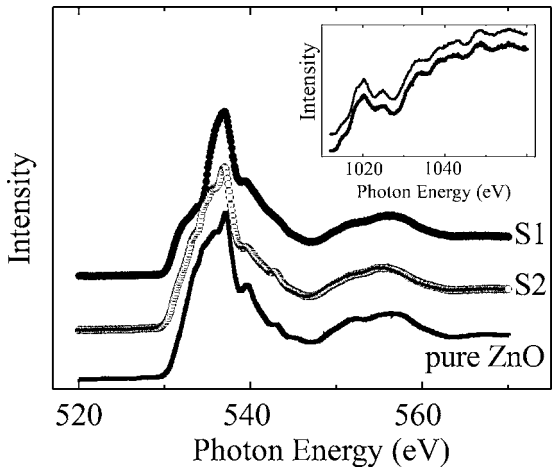

FIG. 7. O *K* edge XAS spectra of an undoped reference ZnO sample (black line), the $Zn_{0.9}Co_{0.1}O$ sample *S*1 (closed circles), and the $Zn_{0.9}Co_{0.1}O$ sample *S*2 (open circles). The inset shows a comparison of the Zn $L_{2,3}$ edge XAS spectra of pure ZnO (black line) and the $Zn_{0.9}Co_{0.1}O$ sample *S*1 (closed circles).

represents off-resonance ($h\nu$=774 eV) and on-resonance ($h\nu$=777 eV) valence band photoemission spectra of sample *S*1. The difference spectrum shown in Fig. 6(b) was obtained by subtraction of the off- and on-resonance and can be related to the partial density of states (PDOS) of Co in the valence band of ZnO. Figure 6(c) shows off- and on-resonance PES spectra from sample *S*2 and the corresponding PDOS is shown in Fig. 6(d). In Figs. 6(a) and 6(c), the intensities of the off-resonance spectra were normalized to those of the on-resonance spectra at 7 eV. Both difference curves are almost identical with a sharp peak at about 3.5 eV of BE which is in good agreement with previous studies.[14,38] These results show that in ferromagnetic (*S*1) as well as in paramagnetic (*S*2) Co-doped ZnO samples the Co 3*d* states are located near the top of the valence band at about 3.5 eV of binding energy. Recent local spin density approximation calculations performed for Co-doped ZnO[40] show that within the LSDA+*U* scheme (U=4.5 eV) the Co 3*d* PDOS is localized around 3.5 eV in the valence band of ZnO in agreement with our measurements. However, in this model Co doping yielded no tendency to ferromagnetic ordering. Moreover, the calculated ground state for the case of substitutional magnetic transition-metal ions combined with oxygen vacancies was found to be antiferromagnetic.[40]

In order to provide the evidence that ferromagnetic behavior in Co-doped ZnO is donor carrier mediated and thus can be explained in the frame of the BMPs model,[4] a direct relationship between the amplitude of measured M_s and the oxygen vacancies concentration of different samples should be established. Here we used O *K* edge XAS measurements on both sets of samples (*S*1 and *S*2) to probe the local structure of Co-doped ZnO and especially the oxygen-related defects in the ZnO host lattice. Figure 7 shows the comparison of O *K* edge XAS spectra from the undoped reference ZnO sample, the $Zn_{0.9}Co_{0.1}O$ sample *S*1, and the $Zn_{0.9}Co_{0.1}O$ sample *S*2. The spectral line shape of the O *K* edge agrees well with the XAS spectra obtained from ZnO powder,[41] PLD grown Co-doped ZnO,[42] and chemical vapor deposition prepared samples.[43] The region between 530 and 538 eV can be attributed to the hybridization between O 2*p* and Zn 4*s* states followed by the region between 539 and 550 eV which is due to the hybridization between O 2*p* and Zn 4*p* states. Above 550 eV the spectrum can be assigned to the hybridization between O 2*p* and Zn 4*d* states. The broadening of the spectral features observed in the *S*1 sample in comparison with the sample *S*2, as well as to the undoped reference ZnO sample at 537, 540, and 543 eV, was recently assigned to the presence of the oxygen vacancies[42] showing that the oxygen-related defect concentration in sample *S*1 is higher than in sample *S*2. Zn $L_{2,3}$ XAS spectra shown in the inset of Fig. 7 are in agreement with the XAS measurements at ZnO nanorods[44] and crystalline ZnO[45] corroborating that no significant Zn defect related features such as Zn interstitials are present in the samples. The spectroscopic measurements show that oxygen vacancies or oxygen related defects rather dominate than Zn interstitials. In particular, the oxygen vacancies concentration in *S*1 samples is higher than in the *S*2 samples, as well as in the ZnO reference sample confirming that in the presented samples a specific variation of oxygen vacancies was achieved. Moreover, magnetic and spectroscopic data presented here imply that the oxygen vacancies concentration in Co-doped ZnO is strongly correlated with the observed ferromagnetism confirming the central hypothesis of the spin-split impurity band model proposed by Coey *et al.*,[4] namely that ferromagnetism depends strongly on the oxygen vacancy constituted BMPs. Within the BMPs model, the higher density of oxygen vacancies yields to a larger overall volume occupied by BMPs, thus increasing their probability of overlapping and, therefore, incorporating more Co ions into ferromagnetic areas and enhancing ferromagnetism. Here, we note that although carriers (donor electrons) are implicated in the BMPs model, this analysis does not

imply macroscopic conductivity. The magnetic phase diagrams for defect-induced ferromagnetism in ZnO DMS may possess a region in which the material is both insulating and ferromagnetic.[4]

IV. CONCLUSION

In conclusion, we prepared epitaxial $Zn_{1-x}Co_xO$ films with $0.05 < x < 0.1$ by means of a magnetron sputtering technique. XRD measurements show that the Co-doped ZnO films have a single-phase wurtzite structure without any impurity phases. Two different preparation routes, i.e., sputtering in Ar atmosphere and sputtering in Ar/O_2 atmosphere in conjunction with a postannealing step, were implemented in order to control the concentration of oxygen vacancies in the ZnO host lattice. Magnetization measurements indicate ferromagnetic behavior at low temperatures for the samples prepared in oxygen-poor conditions whereas the samples prepared in oxygen-rich conditions show extremely small if any ferromagnetic signal giving a clear evidence that ferromagnetism in the $Zn_{1-x}Co_xO$ samples is related to preparation conditions. Co $L_{2,3}$ XAS together with optical transmittance measurements show that in both sets of samples (ferromagnetic as well as paramagnetic) Co ions are present in the high-spin Co^{2+} state under tetrahedral symmetry indicating a proper incorporation in the ZnO host lattice. The spectroscopic data show that the presence of Co^{2+} ions is essential but not an sufficient condition for the ferromagnetism in Co-doped ZnO. Comparison of the O *K* edge XAS spectra of the samples sputtered in oxygen-poor and oxygen-rich conditions show substantial changes in the spectral line shape which are attributed to the presence of lattice defects such as oxygen vacancies in the ferromagnetic oxygen-poor Co-doped ZnO samples. Our findings indicate that ferromagnetic properties of the Co-doped ZnO samples are strongly correlated with the presence of the oxygen vacancies in the ZnO lattice supporting the spin-split impurity band model.

ACKNOWLEDGMENTS

E.B. and M.F. acknowledge the cooperation with A. Barth for SQUID measurements and financial support by BESSY (Berlin). This work was supported by the Landesstiftung Baden-Württemberg "Kompetenznetz Nanostrukturen," Teilprojekt C10. Part of this work was supported by SFB 513.

[1]H. Ohno, Science **281**, 951 (1998).
[2]T. Dietl, H. Ohno, F. Matsukura, J. Cibert, and D. Ferrand, Science **287**, 1019 (2000).
[3]T. Dietl, H. Ohno, and F. Matsukura, Phys. Rev. B **63**, 195205 (2001).
[4]J. M. D. Coey, M. Venkatesan, and C. B. Fitzgerald, Nat. Mater. **4**, 173 (2005).
[5]K. Ueda, H. Tabata, and T. Kawai, Appl. Phys. Lett. **79**, 988 (2001).
[6]C. Song, K. W. Geng, F. Zeng, X. B. Wang, Y. X. Shen, and F. Pan, Phys. Rev. B **73**, 024405 (2006).
[7]M. Venkatesan, C. B. Fitzgerald, J. G. Lunney, and J. M. D. Coey, Phys. Rev. Lett. **93**, 177206 (2004).
[8]T. Fukumura, Z. Jin, M. Kawasaki, T. Shono, T. Hasegawa, S. Koshihara, and H. Koinuma, Appl. Phys. Lett. **78**, 958 (2001).
[9]W. Jung, S.-J. An, G.-C. Yi, C. U. Jung, S.-I. Lee, and S. Cho, Appl. Phys. Lett. **80**, 4561 (2002).
[10]B. Martínez, F. Sandiumenge, L. Balcells, J. Arbiol, F. Sibieude, and C. Monty, Phys. Rev. B **72**, 165202 (2005).
[11]S. Yin *et al.*, Phys. Rev. B **73**, 224408 (2006).
[12]G. Lawes, A. Risbud, A. P. Ramirez, and R. Seshadri, Phys. Rev. B **71**, 045201 (2005).
[13]J. H. Kim, H. Kim, D. Kim, Y. E. Ihm, and W. K. Choo, J. Appl. Phys. **92**, 6066 (2002).
[14]S. C. Wi *et al.*, Appl. Phys. Lett. **84**, 4233 (2004).
[15]K. Sato and H. Katayama-Yoshida, Phys. Status Solidi B **229**, 673 (2002).
[16]H. Weng, X. Yang, J. Dong, H. Mizuseki, M. Kawasaki, and Y. Kawazoe, Phys. Rev. B **69**, 125219 (2004).
[17]J. E. Jaffe, T. C. Droubay, and S. A. Chambers, J. Appl. Phys. **97**, 073908 (2005).
[18]K. R. Kittilstved, W. K. Liu, and D. R. Gamelin, Nat. Mater. **5**, 291 (2006).
[19]K. R. Kittilstved, D. A. Schwartz, A. C. Tuan, S. M. Heald, S. A. Chambers, and D. R. Gamelin, Phys. Rev. Lett. **97**, 037203 (2006).
[20]N. H. Hong, J. Sakai, N. T. Huong, N. Poirot, and A. Ruyter, Phys. Rev. B **72**, 045336 (2005).
[21]H. S. Hsu *et al.*, Appl. Phys. Lett. **88**, 242507 (2006).
[22]H. Ohno, H. Munekata, T. Penney, S. von Molnár, and L. L. Chang, Phys. Rev. Lett. **68**, 2664 (1992).
[23]A. Kaminski and S. Das Sarma, Phys. Rev. Lett. **88**, 247202 (2002).
[24]P. A. Wolff, R. N. Bhatt, and A. C. Durst, J. Appl. Phys. **79**, 5196 (1996).
[25]J. H. Park, M. G. Kim, H. M. Jang, S. Ryu, and Y. M. Kim, Appl. Phys. Lett. **84**, 1338 (2004).
[26]D. C. Reynolds, D. C. Look, B. Jogai, and T. C. Collins, Appl. Phys. Lett. **79**, 3794 (2001).
[27]D. C. Reynolds, D. C. Look, B. Jogai, C. W. Litton, T. C. Collins, W. Harsch, and G. Cantwell, Phys. Rev. B **57**, 12151 (1998).
[28]S. A. Studenikin and M. Cocivera, J. Appl. Phys. **91**, 5060 (2002).
[29]P. S. Xu, Y. M. Sun, C. S. Shi, G. F. Q. Xu, and H. B. Pan, Nucl. Instrum. Methods Phys. Res. B **199**, 286 (2003).
[30]H. S. Kang, J. S. Kang, J. W. Kim, and S. Y. Lee, J. Appl. Phys. **95**, 1246 (2004).
[31]K. Vanheusden, C. H. Seager, W. L. Warren, D. R. Tallant, and J. A. Voigt, Appl. Phys. Lett. **68**, 403 (1996).
[32]P. Koidl, Phys. Rev. B **15**, 2493 (1977).
[33]A. Dinia, G. Schmerber, C. Mény, V. Pierron-Bohnes, and E. Beaurepaire, J. Appl. Phys. **97**, 123908 (2005).
[34]D. Mao-Lu and Z. Min-Guang, J. Phys. C **21**, 1561 (1988).
[35]*Optical Processes of Semiconductors*, edited by J. I. Pankove (Prentice-Hall, Engelwood Cliffs, NJ, 1971).
[36]K. J. Kim and Y. R. Park, Appl. Phys. Lett. **81**, 1420 (2002).
[37]K. Samanta, P. Bhattacharya, and R. S. Katiyar, Appl. Phys. Lett. **87**, 101903 (2005).
[38]M. Kobayashi *et al.*, Phys. Rev. B **72**, 201201(R) (2005).
[39]J. Okabayashi *et al.*, J. Appl. Phys. **95**, 3573 (2004).
[40]P. Gopal and N. A. Spaldin, Phys. Rev. B **74**, 094418 (2006).
[41]C. McGuinness, C. B. Stagarescu, P. J. Ryan, J. E. Downes, D. Fu, K. E. Smith, and R. G. Egdell, Phys. Rev. B **68**, 165104 (2003).
[42]S. Krishnamurthy *et al.*, J. Appl. Phys. **99**, 08M111 (2006).
[43]J. W. Chiou *et al.*, Appl. Phys. Lett. **89**, 043121 (2006).
[44]J. W. Chiou *et al.*, Appl. Phys. Lett. **85**, 3220 (2004).
[45]J.-H. Guo, L. Vayssieres, C. Persson, R. Ahuja, B. Johansson, and J. Nordgren, J. Phys.: Condens. Matter **14**, 6969 (2002).